

Electrical and optical characterization of metastable deep-level defects in GaAs

W. R. Buchwald, G. J. Gerardi, and E. H. Poindexter

Electronics Technology and Devices Laboratory, Fort Monmouth, New Jersey 07703-5000

N. M. Johnson

Xerox Palo Alto Research Center, Palo Alto, California 94304

H. G. Grimmeiss

Department of Solid State Physics, University of Lund, S-220 07 Lund, Sweden

D. J. Keeble

Department of Physics, Michigan Technological University, Houghton, Michigan 49931

(Received 9 November 1988; revised manuscript received 15 March 1989)

Two metastable defect configurations, here designated $M3$ and $M4$, are observed in n -type GaAs grown by metal organic chemical-vapor deposition. The configurations are comprehensively characterized by deep-level transient spectroscopy and have enthalpies for thermal emission of electrons of 0.6 and 0.3 eV, respectively. The metastable transformation between these two centers is found to be temperature induced and bias controlled. The capture cross sections for both defect configurations are found to be temperature independent with values of 5.1×10^{-18} and 1.8×10^{-18} cm² for the $M3$ and $M4$ configurations, respectively. Defect depth profiling shows defect densities that decrease monotonically from approximately 1×10^{13} cm⁻³ at 0.2 μ m below the surface to approximately 1×10^{11} cm⁻³ at 0.6 μ m below the surface for both defect configurations. Photocapacitance measurements give photoionization threshold energies consistent with the electrical measurements and photoionization cross sections of about 2×10^{-19} cm² at a photon energy of 0.75 eV. The complete metastable reaction kinetics are also reported, as well as the electric field dependence of the emission rate for each configuration.

I. INTRODUCTION

Defect metastability has been reported in a variety of semiconducting materials.¹⁻⁹ This paper presents a comprehensive characterization of a recently reported metastable defect found in n -type GaAs grown by metalorganic chemical-vapor deposition (MOCVD).⁹ This metastable defect produces two distinct peaks in a deep-level transient (DLTS) spectrum¹⁰ which depend on the heat-treatment and biasing conditions used prior to measurement. If the sample is heated to 400 K under a zero bias, DLTS reveals two deep levels with activation energies for thermal emission of electrons of 0.6 and 0.83 eV. If, however, the same heat treatment is applied with a reverse bias, two deep levels are observed with activation energies for thermal emission of electrons of 0.3 and 0.83 eV. The 0.83-eV level is an electron trap and is most probably the $EL2$ center commonly found in this material; it is not the subject of this investigation. The 0.6- and 0.3-eV levels, labeled $M3$ and $M4$ here, respectively, are proposed to be associated with one defect center that undergoes a configurational transformation. The transformation process is found to be completely reversible; thus, these defects are considered to be metastable centers. This paper extends the characterization of these defect centers and presents metastable reaction kinetics, capture cross-section data, field-effect data, and photoionization cross-section data.

II. SAMPLES AND INITIAL CHARACTERIZATION

The samples studied in this work were n -type GaAs films grown by MOCVD on n^+ -type substrates. The material was intentionally doped with Si to a uniform concentration of 8.0×10^{15} cm⁻³. The GaAs was encapsulated *in situ* with a silicon nitride layer to reduce the possibility of As out-diffusion from the surface during subsequent processing. The back surfaces of the wafers were coated with Au-Ge films and alloyed to form Ohmic contacts. After removal of the nitride layer, 0.5-mm-diam Pt electrodes were deposited on the front surface through a shadow mask to form Schottky-barrier diodes.

Data were obtained with a Polaron S4600 DLTS measurement system and a Hewlett-Packard HP9826 computer. The software supplied by Polaron was modified to improve signal averaging, and new software was written to perform the thermally stimulated capacitance experiments. The capacitance meter supplied with the Polaron system, a Boonton 72-4B, was factory modified for short response times. The DLTS capacitance transients were analyzed with the sample-and-hold circuitry contained in the Polaron system, with the diode mounted in the Polaron liquid-nitrogen-cooled cryostat. A Kratos Analytical single-grating monochromator and vacuum spectrometer with suitable-order sorting filters was used for the determination of the photoionization thresholds and cross sections. The material had previously been characterized by

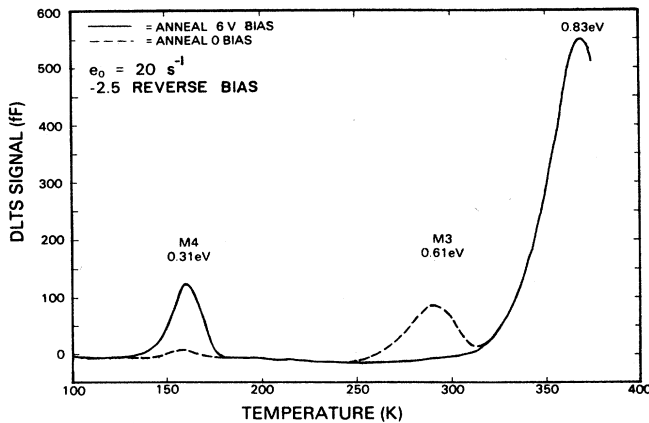


FIG. 1. DLTS spectra for Schottky-barrier diodes on *n*-type, as-grown, MOCVD GaAs after selected bias-temperature anneals.

photoluminescence.¹¹

Figure 1 presents DLTS spectra which confirm the metastable nature of the levels labeled *M3* and *M4*. Care was taken to ensure that the temperature cycling and rate window did not alter the concentration of defects in each metastable state. From Arrhenius analysis of similar spectra recorded over a range of emission-rate windows, it was determined that the electron-emission rates of the *M3* and *M4* centers could be defined by the following parametrized expressions.

$$M3: e(T) = 7.2 \times 10^6 T^2 \exp[(-0.61 \text{ eV})/kT],$$

$$M4: e(T) = 3.3 \times 10^6 T^2 \exp[(-0.31 \text{ eV})/kT].$$

The estimated error for the activation energies in electron emission was ± 0.005 eV. The defect concentrations, capture cross sections, and effect of applied field will be discussed in later sections. Figure 2 presents the Arrhenius plots used to obtain the above values. The voltage pulse used to obtain the capacitance transients was a reverse

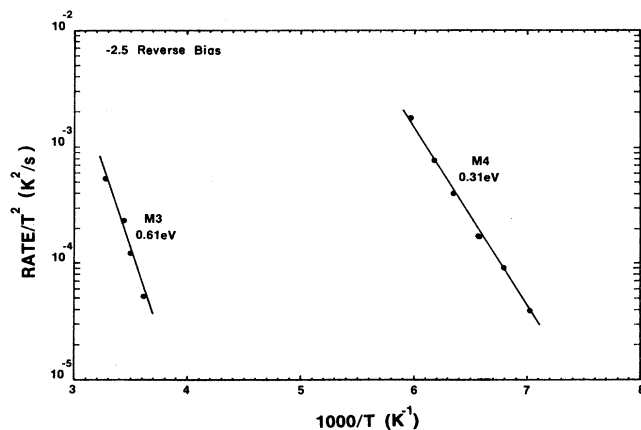


FIG. 2. Arrhenius analysis of DLTS data obtained from metastable centers found in *n*-type MOCVD-grown GaAs.

bias of 2.5 V followed by a fill pulse to 0 V for approximately 1 ms.

III. METASTABLE REACTION KINETICS

The data in Fig. 3 represent the defect concentration of each defect center after a 12-min isochronal anneal at the indicated temperature. The sample was always treated to maximize the concentration of one particular defect configuration prior to performing the 12-min anneal. The solid line represents the actual data fit to the data. The data fit was obtained by assuming the defect concentration $N(t, T)$ for defect formation and annealing followed the functional forms

$$N(t, T) = N_0 \{1 - \exp[-te_0(T)]\} \quad (1)$$

and

$$N(t, T) = N_0 \exp[-te_0(T)], \quad (2)$$

respectively. In the above equations, N_0 is the maximum defect concentration, t is time in seconds, and $e_0(T)$ is the rate of transformation as a function of temperature. The rate of transformation is assumed to take the form

$$e_0 = \alpha \exp(-E/kT), \quad (3)$$

where T is the temperature in K, k is Boltzmann's constant, α is a prefactor with units of s^{-1} , and E is the energy barrier for the transformation of the defect configuration. The method used to extract the energy barrier for configurational transformation differed from the approach used by other investigators^{1,2} in that isothermal anneals were not performed. Prior to performing any isochronal anneal, the sample was always treated to maximize one particular defect concentration. In this way, N_0 was precisely known, thus minimizing the error associated with the determination of the energy barrier E . It was determined that a 20-min anneal at 400 K, either under a 6-V reverse bias, or a zero bias, maximized the concentration of the *M4* or *M3* defect center, respectively. The defect concentration was experimentally confirmed by performing a DLTS scan after successive, identical, DLTS scans verified that the DLTS scan itself did not change the defect concentration. Figure 4 represents the extraction of the value for the energy barrier associated with the formation of the *M4* center using the method described above. The energy for the decay of the *M3* center and the formation of the *M4* center was found to be 1.70 ± 0.08 eV, while the energy needed for the decay of the *M4* center and the formation of the *M3* center was found to be 0.8 ± 0.08 eV. The decay energies quoted here differ slightly from those quoted in Ref. 9, which did not take into account a small baseline drift in the DLTS signal. For completeness, the prefactors in Eq. (3) were determined, and found to be 10^{21} for the formation of the *M4* center and the decay of the *M3* center, and 10^7 for the formation of the *M3* center and decay of the *M4* center.

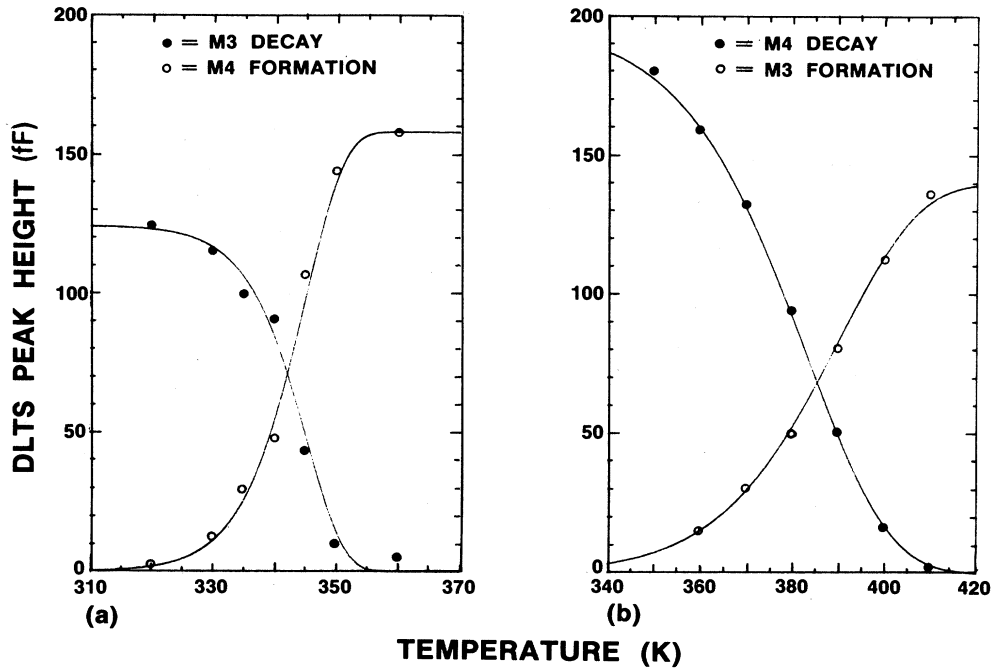


FIG. 3. DLTS peak heights for the $M3$ and $M4$ centers in GaAs after 12-min isochronal anneals at the indicated temperatures under (a) 6-V reverse bias and (b) zero bias. The solid lines represent actual data fits using equations given in text.

IV. DEPTH PROFILES

In order to accurately determine the defect concentration, defect densities as functions of depth below the surface were calculated by the double-correlation DLTS technique (DDLTS).³ In DDLTS, the subtraction of two DLTS signals with slightly different fill-pulse amplitudes defines a narrow, spatial observation window within the depletion region of the diode. The DDLTS signal relates to the defect density only within this window; thus, a depth profile of the defect concentration is obtained. When calculating the defect densities, the point at which

the defect level falls below the quasi-Fermi level, and also the depletion width as a function of temperature, were taken into account. In Fig. 5, the results of the defect depth profiling show virtually identical values for the $M3$ and $M4$ defect centers. As can be seen, the majority of the defects are located within 0.6 μm of the surface.

V. CAPTURE CROSS SECTIONS

In general, the emission rate of a defect center can be given by¹⁴⁻¹⁸

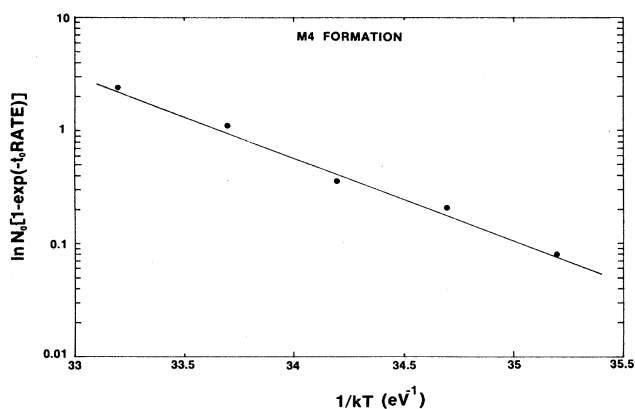


FIG. 4. Extraction of energy barrier associated with the formation of the $M4$ metastable defect center.

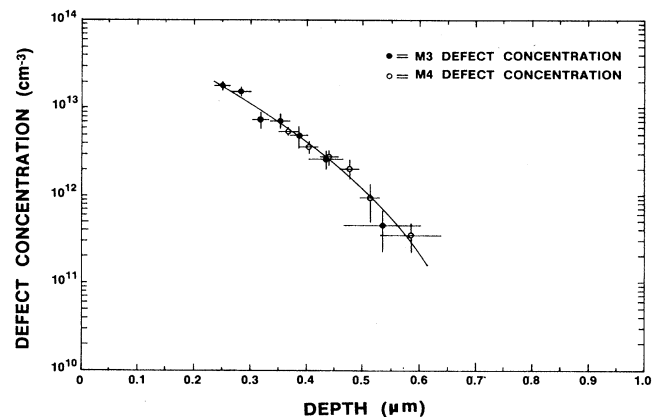


FIG. 5. DDLTS depth profiling for the $M3$ and $M4$ metastable centers.

$$e = \gamma T^2 \exp(\Delta S/k) \exp[-(\Delta H + E_\sigma)/kT], \quad (4)$$

where γ is a temperature-independent constant,¹⁸ T is the temperature in K, k is Boltzmann's constant, ΔS is the change in entropy of the system, ΔH is the change in enthalpy, and E_σ is an energy barrier to carrier capture. From this it is clear that an Arrhenius plot of e/T^2 will give a value for the thermal activation energy (obtained from a DLTS experiment) given by

$$E_{\text{DLTS}} = E_\sigma + \Delta H. \quad (5)$$

Therefore, in order to obtain a value for the change in enthalpy, it must be determined if the capture process has an energy barrier associated with it. An energy-dependent capture process can take the form

$$\sigma(T) = \sigma_\infty \exp(-E_\sigma/kT). \quad (6)$$

Thus, it is necessary to determine the temperature dependence of the capture process. The rate of carrier capture c is given by the equation¹⁸

$$c = \langle v_{\text{th}} \rangle \sigma n, \quad (7)$$

where n is the free-carrier concentration and $\langle v_{\text{th}} \rangle$ is the mean thermal velocity of the carriers. In order to extract the capture rate, the pulse-train method was used.¹⁹ With this method, the sample was reverse biased at a high temperature to empty any trapped electrons; then, still under a reverse bias, it was cooled down to a temperature low enough such that the defect center being studied would not emit any captured carriers. Short, undistorted, zero-bias filling pulses of known duration were then applied to the sample and the change in sample capacitance monitored, which determined the rate of carrier capture. The switching circuit described in Ref. 18 was used to disconnect the capacitance meter from the circuit before the filling pulse was applied, which allows the sample to be pulsed with a distortion-free signal. Trap filling in the Debye-tail region of the diode depletion width is known to introduce a slow component into the measured change

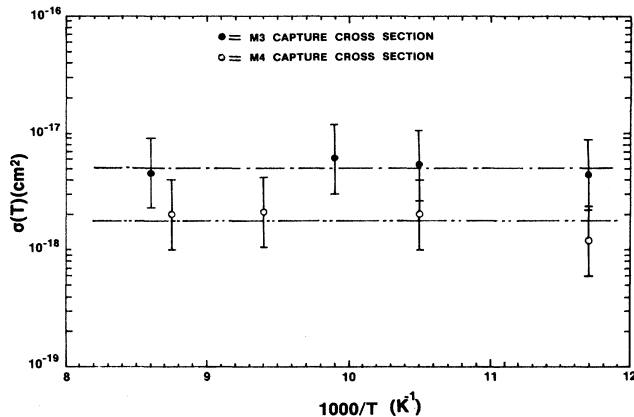


FIG. 6. Capture cross-section temperature dependence for the $M3$ and $M4$ metastable defect configurations.

in capacitance during trap-filling experiments.²⁰⁻²² In this work, the capacitance signal was dominated by the slower Debye-tail filling because the majority of the defects were located near the surface of the diode as determined by DDLTS depth profiling. The faster filling rate was used in the determination of the capture cross section.

Figure 6 shows the results of these capture cross-section measurements. As can be seen, both centers have a temperature-independent capture cross section with values of $5.1 \times 10^{-18} \text{ cm}^2$ and $1.8 \times 10^{-18} \text{ cm}^2$ for the $M3$ and $M4$ configurations, respectively.

VI. FIELD EFFECTS

It is well known that, for certain centers, the electron emission rate is enhanced due to an applied electric field according to the relation^{23,24}

$$\ln e(\mathcal{E}, T) = \ln e(0, T) + (\beta/kT)\mathcal{E}^{1/2}, \quad (8)$$

where \mathcal{E} is the magnitude of the electric field $\beta = q(q/\pi\epsilon)^{1/2}$, and ϵ is the dielectric constant of the material. This emission enhancement is due to the emitted electron experiencing a Coulombic attraction with the defect core and is known as the Poole-Frenkel effect. Figure 7 shows the results of applied electric field on the emission rate of the $M3$ center. The proportionality constant between emission rate and electric field β for the $M3$ center was found to be $3.0 \times 10^{-4} (\text{V cm})^{1/2}$, in good agreement with the one-dimensional (1D) Poole-Frenkel theoretical calculations of $2.1 \times 10^{-4} (\text{V cm})^{1/2}$ for a single donor and $2.9 \times 10^{-4} (\text{V cm})^{1/2}$ for a double donor. No field effect was observed for the $M4$ center. In the past, the Poole-Frenkel effect has been used for the unambiguous determination of donorlike versus acceptorlike nature of a defect. Recent work, however,²⁵ suggests that short-range perturbations to the long-range Coulombic tail, such as an energy barrier to carrier capture, can dramatically decrease the effect of applied fields on

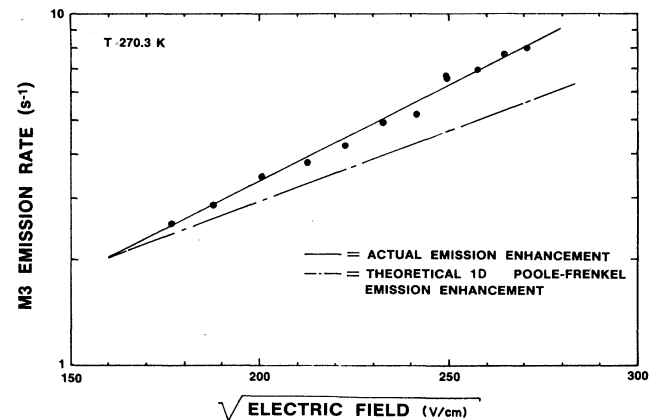


FIG. 7. Emission-rate enhancement for the $M3$ defect center as a function of applied electric field. The dotted line represents theoretical one-dimensional Poole-Frenkel emission enhancement for a double donor.

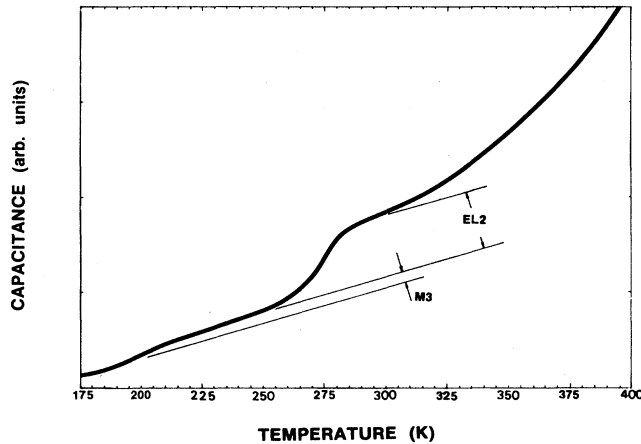


FIG. 8. TSCAP scan indicating electron emission from the *M3* and *E12* centers, but no emission during the *M3* to *M4* metastable transformation.

Coulombic centers. Thus, a null result for the Poole-Frenkel effect does not unambiguously determine its type. In this work, because no short-range effects were observed for the *M4* center, as well as no Poole-Frenkel effect, the center is considered to be acceptorlike. It should be noted that in order to obtain accurate results for the field-enhancement experiments, DDLTS was used and the spatial observation window kept small in order to obtain a very accurate value for the field affecting the emitting centers. From these data, the activation energy for the *M4* center is found to be 0.31 eV independent of electric field. The *M3* center has an activation energy of 0.61 eV under a reverse bias of 2.5 V.

VII. THERMALLY STIMULATED CAPACITANCE

In order to determine if a change in charge state accompanies the metastable transformation from the *M3* state to the *M4* state, a TSCAP experiment was performed.¹ The sample was initially treated to maximize the *M3* defect concentration. Under zero bias the sample was then cooled to 175 K. A reverse bias of 4 V was then applied to the sample and the sample slowly warmed as the capacitance was monitored. It was determined independently that a heating rate of 1.5×10^{-2} K/s was slow enough that all of the defects converted from the *M3* state to the *M4* state by the time the sample reached 400 K. The results of this procedure are shown in Fig. 8. Steps in the capacitance curve are clearly seen at 200 K (*M3* emission) and 275 K (*EL2* emission). No capacitance change is observed at temperatures greater than 275 K. It is therefore concluded that no change in charge state accompanies the *M3* to *M4* metastable transformation.

VIII. PHOTOIONIZATION CROSS SECTIONS

The photoionization threshold energies and the photoionization cross sections were determined for each metastable configuration by measuring the change in the diode

capacitance as a function of incident-light energy. If the rate of light-induced capacitance change can be determined, the photoionization cross section is known via the relation²⁶

$$e_0 = \sigma_0 \phi, \quad (9)$$

where σ_0 is the photoionization cross section and ϕ is the photon flux at the defect site. The initial-slope technique was used for the determination of the photoionization cross section.²⁶ Photoionization measurements were performed at 85 K. In the case of the *M3* configuration, a zero-bias filling pulse was used for initial filling of all defect centers with electrons. For the *M4* center, white light was used for the initial populating of all centers. After trap filling, a reverse bias was applied to the diode to place a portion of the filled defects above the Fermi level. Monochromatic light of known wavelength and intensity was then used to illuminate the sample. Once the defect threshold energy was reached, a capacitance increase was observed as trapped electrons were emitted to the conduction band. The initial slope of this capacitance transient was measured as a function of incident-light energy. The entire transient was observed for an incident-light energy of 0.9 eV in order to obtain the electron emission rate and thus fix the absolute value of the photoionization cross section. A calibrated thermopile was used to obtain the absolute value of the incident-light intensity at 0.9 eV. The results of these measurements are shown in Fig. 9. As can be seen, the *M3* configuration gives a threshold energy of 0.55 eV and the *M4* configuration a threshold energy of 0.35 eV in good agreement with electrical data. The absolute value of the photoionization cross section in both configurations at an incident-light energy of 0.75 eV is approximately 2×10^{-19} cm². The thresholds at greater than 0.8-eV light energy are believed to be *EL2* related.

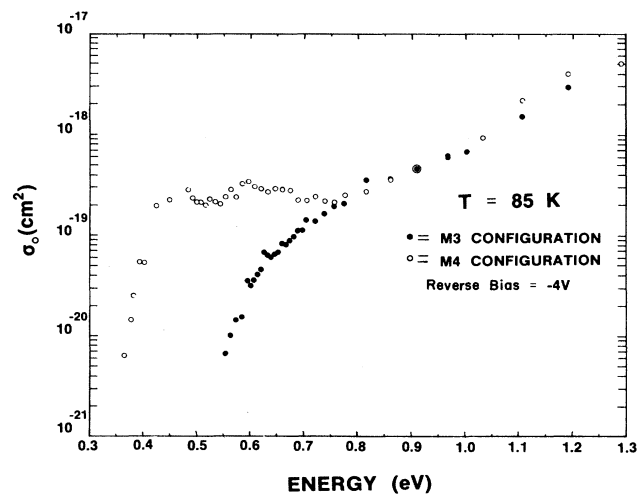
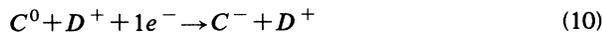


FIG. 9. Photoionization cross sections as determined via the initial slope technique for the *M3* and *M4* metastable defect configurations found in *n*-type, MOCVD-grown GaAs. The measurements were made at 85 K under 4 V reverse bias.

IX. CONCLUSION

It seems clear from the similarities between decay and formation energies, as the system goes from the $M3$ to the $M4$ state and *vice versa*, as well as the almost identical depth profiles, that the $M3$ and $M4$ centers are one and the same defect undergoing a configurational change. Due to the temperature needed for the transformation to occur, a large lattice relaxation is one possible mechanism. Because the defect appears in the near-surface region, one might guess that it is stress related due to the nitride encapsulation or that the nitride capping trapped a bulk constituent near the surface that might otherwise have diffused out during processing. Of course, electrical characterization alone will not determine the chemical nature of a defect system; nevertheless, a tentative model is proposed which does account for the key features of the experimental evidence. This model is similar to models proposed for other metastable centers and relies on the pairing of a native acceptor or defect complex C^0 and a shallow donor D^+ .^{1,3} This process is electrostatically driven, and may be represented as follows

$M4$ to $M3$ transition (zero-bias required):



In the above model the C^- defect could be considered the $M4$ center of this paper. Once a sufficiently high temperature is reached, and the sample is zero biased to

keep the deep $M4$ center filled, and because D^+ is a shallow donor, hence positive, then Coulombic attraction causes the C^- and the D^+ center to relax together forming the $(CD)^0$ complex as shown in Eq. (11). This $(CD)^0$ complex could be considered the $M3$ configuration. The reverse process can similarly be shown as follows.

$M3$ to $M4$ (reverse bias):



High temperatures and reverse bias to keep the C^0 state empty allow the donor and the complex to relax into a separate condition. This model is attractive in that it allows the $M4$ center to be an acceptor and the $M3$ center to be a donor—the configurational change does not liberate an electron. Also, there is a driving force behind the lattice relaxation, namely, Coulombic attraction. This model should, however, be considered tentative, even though it accounts for a majority of the data. As has been stated previously, electrical characterization alone cannot be used for physicochemical modeling of a defect species.

ACKNOWLEDGMENTS

The authors of this paper would like to thank L. Tilly for his assistance with the measurements of the photoionization cross sections for the $M4$ configuration.

-
- ¹M. Levinson, J. L. Benton, and L. C. Kimerling, *Phys. Rev. B* **27**, 6216 (1983).
²M. Levinson, M. Stavola, J. L. Benton, and L. C. Kimerling, *Phys. Rev. B* **28**, 5848 (1983).
³M. Levinson, M. Stavola, P. Besomi, and W. A. Bonner, *Phys. Rev. B* **30**, 5817 (1984).
⁴M. Levinson, *J. Appl. Phys.* **58**, 2628 (1985).
⁵G. E. Jellison, Jr., *J. Appl. Phys.* **58**, 5715 (1982).
⁶A. Chantra and D. Bois, *Phys. Rev. B* **31**, 7979 (1985).
⁷M. Levinson, *Phys. Rev. B* **28**, 3660 (1983).
⁸A. Sibille and A. Mircea, *Phys. Rev. Lett.* **47**, 142 (1981).
⁹W. R. Buchwald, N. M. Johnson, and L. P. Trombetta, *Appl. Phys. Lett.* **50**, 1007 (1987).
¹⁰D. Lang, *J. Appl. Phys.* **45**, 3023 (1974).
¹¹B. Street, N. M. Johnson, and R. D. Burnham, *Mater. Res. Soc. Symp. Proc.* **46**, 333 (1985).
¹²H. Lefevre and M. Schulz, *Appl. Phys.* **12**, 45 (1977).
¹³C.-O. Almladh and G. H. Reese, *J. Phys. C* **14**, 4575 (1981).
¹⁴N. M. Johnson, in *Materials Characterization*, edited by N. W. Cheung and M.-A. Nicolet (Materials Research Society, Pittsburgh, 1986), pp. 75–94.
¹⁵J. A. VanVechten and C. D. Thurmond, *Phys. Rev. B* **14**, 3539 (1978).
¹⁶O. Engstrom and A. Alm, *Solid State Electron.* **21**, 1571 (1978).
¹⁷A. Mitonnaue, A. Mircea, G. M. Martin, and D. Pons, *Rev. Phys. Appl.* **14**, 853 (1979).
¹⁸G. Martin, A. Mitonnaue, and A. Mircea, *Electron. Lett.* **13**, 191 (1977).
¹⁹H. G. Grimmeiss and C. Ovren, *J. Phys.* **14**, 1032 (1981).
²⁰A. Zylbersztejn, *Appl. Phys. Lett.* **33**, 200 (1978).
²¹D. Pons, *J. Appl. Phys.* **55**, (1984).
²²J. M. Noras and H. R. Szawalska, *J. Phys. C* **15**, 200 (1982).
²³J. Frankel, *Phys. Rev.* **54**, 647 (1938).
²⁴L. C. Kimerling and J. L. Benton, *Appl. Phys. Lett.* **39**, 411 (1981).
²⁵W. R. Buchwald and N. M. Johnson, *J. Appl. Phys.* **64**, 958 (1988).
²⁶H. G. Grimmeiss and B. Skarstam, *Phys. Rev. B* **23**, 1947 (1981).